

# CONTROL PROCEDURES TO CHECK THE $\sigma$ -W RELATIONSHIP USED TO DESIGN A SFRC SLAB

*P. Martinelli<sup>1</sup>, M. Colombo<sup>2</sup>, M. Tratta<sup>3</sup>, D. Trentini<sup>4</sup>, S. Cavalaro<sup>5</sup>, A. de la Fuente<sup>6</sup>, A. Aguado<sup>7</sup>, M. di Prisco<sup>8\*</sup>*

<sup>1</sup> Assistant Professor, Politecnico di Milano, paolo.martinelli@polimi.it

<sup>2</sup> Assistant Professor, Politecnico di Milano, matteo.colombo@polimi.it

<sup>3</sup> Structural Engineer, Politecnico di Milano, matteo.tratta@mail.polimi.it

<sup>4</sup> Structural Engineer, Politecnico di Milano, davide.trentini@mail.polimi.it

<sup>5</sup> Associate Professor, Universidad Politecnica de Catalunya, sergio.cavalaro@upc.edu

<sup>6</sup> Associate Professor, Universidad Politecnica de Catalunya, albert.de.la.fuente@upc.edu

<sup>7</sup> Professor, Universidad Politecnica de Catalunya, antonio.aguado@nobel.upc.edu

<sup>8\*</sup> Corresponding Author, Professor, Politecnico di Milano, marco.diprisco@polimi.it

## ABSTRACT

In the paper, the reliability of the Model Code approach for evaluating the bearing capacity of a Steel Fiber Reinforced Concrete (SFRC) elevated slab is discussed with reference to the case of a two-stories family house recently built in Italy. To the authors' knowledge, this is the first realization of SFRC elevated slab in Italy. Six standard notched specimens have been cast and tested through a third point bending test set-up. These tests allowed to classify the fiber reinforced material based on post-cracking residual strengths measured for two different crack openings, respectively related to serviceability and ultimate limit states. In conjunction with the SFRC slab casting, four shallow beams (1.5×0.5×0.25 m) having the same thickness of the slab were cast. The shallow beams have been tested in bending to verify the specific bearing capacity of the slab having used for both the slab and the shallow beams the same casting procedure. After the beam tests, coring procedures have been carried out on the shallow beams in order to measure the SFRC tensile behavior. The cored cylinders were tested with two non-standardized indirect tensile methodologies: Double Edge Wedge Splitting (DEWS) and Double Punch (Barcelona) tests.

*Keywords: fiber reinforced concrete (FRC); elevated slab; indirect tensile tests; Barcelona test, DEWS test*

---

Marco di Prisco, PhD, PEng  
Politecnico di Milano  
Department of Civil and Environmental Engineering  
P.za L. da Vinci 32, 20133 Milano  
Italy

Email: marco.diprisco@polimi.it  
Tel: +39 02 2399 8794

## 1. INTRODUCTION

Steel Fiber Reinforced Concrete (SFRC) is a well-known construction material that has been quite extensively used to build redundant structures as for example industrial pavements, pipes, shotcrete linings, tunnel segments, and foundation slabs. The redundancy of these structures makes the use of SFRC particularly convenient because allows significant optimizations of the reinforcement in terms of casting simplification, performance increase (like depth reduction), quality of the casting and durability due to crack opening control. In conjunction with steel fibers, traditional steel high bond bars can be introduced in the critical regions to enhance the robustness of the structures and to activate suitable ductile failure mechanisms at the onset of collapse.

Up to now, the use of SFRC for elevated slabs supported by columns or walls has been very limited and mainly refers to research field [1–4]. A two-stories family house has been recently built in northern Italy using a SFRC elevated slab. To the authors' knowledge, this is the first realization of SFRC foundation and elevated slab in Italy. The building consists of a underground story of 290 m<sup>2</sup>, a SFRC foundation at ground level, 400 mm thick, not indicated in Figure 1 and a slab at ground level of about 240 m<sup>2</sup> realized in SFRC covering the underground story. The SFRC floor has a thickness of 250 mm and behaves as an elevated slab. Figure 1 shows a simplified plan view of the SFRC elevated slab together with the supporting walls and columns.

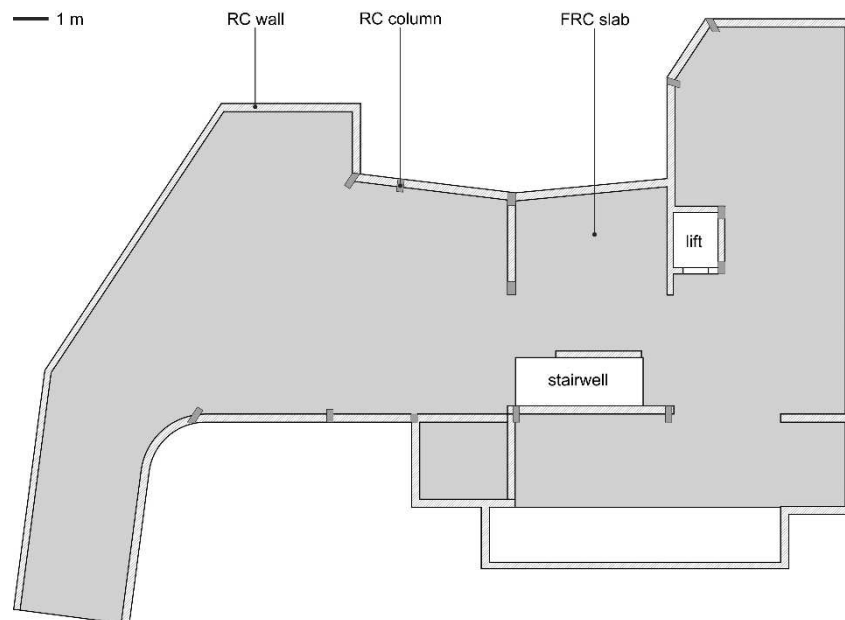


**Figure 1.** SFRC slab plan view.

In the paper, the reliability of the Model Code approach [5] for evaluating the bearing capacity of the SFRC elevated slab is analyzed with reference to the case of the afore-mentioned family house. To this regard, six standard notched specimens (0.55×0.15×0.15 m) were cast and tested through a third point bending test according to [6]. These tests allow to classify the fiber reinforced material based on post-cracking residual strengths measured for two different crack openings, respectively related to serviceability and ultimate limit states. Moreover, in conjunction with the SFRC slab casting, 4 shallow beams (1.5×0.5×0.25 m) having the same thickness of the slab were cast. The shallow beams were tested in bending to verify the specific bearing capacity of the slab having used for both, the slab and the shallow beams, the same casting procedure. Coring procedures have been carried out on the shallow beams in order to measure the SFRC tensile behavior. The cored cylinders were tested with non-standardized indirect tensile methodologies: Double Edge Wedge Splitting (DEWS) and Double Punch (Barcelona) tests [7–8].

## 2. MATERIAL CHARACTERISTICS

The SFRC adopted for the elevated slab has a density equal to 2358 kg/m<sup>3</sup>. The material mix design is specified in Table 1. The fibers used in the mix are low-carbon straight steel fibers, 60 mm long with an aspect ratio ( $l_f/d_f$ ) equal to 60 and a tensile strength higher than 1200 MPa. A fiber content equal to 35 kg/m<sup>3</sup> (.44% by volume) was used.

**Table 1.** SFRC mix design

| Component                      | Dosage (kg/m <sup>3</sup> ) |
|--------------------------------|-----------------------------|
| Cement type CEM II /A-LL 42.5R | 370                         |
| Filler                         | 150                         |
| Gravel                         | 409                         |
| Washed sand                    | 993                         |
| Sifted sand                    | 244                         |
| Water                          | 185                         |
| Super-plasticizer              | 5.6                         |
| Straight steel fiber           | 35                          |

**Table 2.** 3point bending test results: nominal strengths  $f_L$ ,  $f_{R1}$ ,  $f_{R2}$ ,  $f_{R3}$  and  $f_{R4}$  according to EN 14651 [6]

| Reference values   | $f_L$ | $f_{R1}$ | $f_{R2}$ | $f_{R3}$ | $f_{R4}$ |
|--------------------|-------|----------|----------|----------|----------|
|                    | [MPa] | [MPa]    | [MPa]    | [MPa]    | [MPa]    |
| mean ( $m_x$ )     | 5.518 | 4.784    | 4.629    | 4.063    | 3.649    |
| st. dev. ( $s_x$ ) | 0.300 | 1.018    | 1.013    | 0.777    | 0.668    |
| $f_k$ (normal)     | 4.865 | 2.568    | 2.426    | 2.373    | 2.194    |
| $m_y$              | 1.707 | 1.547    | 1.512    | 1.385    | 1.279    |
| $s_y$              | 0.056 | 0.208    | 0.223    | 0.205    | 0.196    |
| $f_k$ (log-normal) | 4.876 | 2.987    | 2.790    | 2.557    | 2.348    |

A fresh state control was carried out according to [9] to determine the fibers quantity in seven different truck mixer used during the slab casting; a mean quantity of fibers equal to 33 kg/m<sup>3</sup> with a coefficient of variation (COV) equal to 20.7% were measured. For each measure of fibers content at fresh state, a cubic compressive test was carried out at 28 days, getting a cubic mean compressive strength equal to 55.6 MPa measured on 150–mm–sided cubic specimens.

The post-peak material tensile behavior was evaluated according to [6] by using a three-point bending test on specimens with a cross-section of 150×150 mm<sup>2</sup> with a 25 mm deep notch and a span of 500 mm. The limit of proportionality  $f_L$ , the residual flexural tensile strengths  $f_{R1}$ ,  $f_{R2}$ ,  $f_{R3}$  and  $f_{R4}$  for a crack mouth opening displacement (CMOD) of 0.5, 1.5, 2.5 and 3.5 mm, respectively, were measured for all the specimens. In Table 2 the average values are reported. The characteristic fracture properties  $f_{Rk}$  are calculated by the well-known expression given in [10] assuming a normal distribution:

$$f_{Rk} = f_{Rm} (1 - k_n V_x) \quad (1)$$

where  $V_x$  is the coefficient of variation of the fracture property considered; it is not known a priori but is estimated from the sample. The factor  $k_n$  is a statistical coefficient that takes into account the number  $n$  of test results of the sample ( $k_n = 2.18$  for  $n = 6$ ). The characteristic fracture properties  $f_{Rk}$  are also calculated by assuming a log-normal distribution following the approach proposed in [10]; the corresponding values are reported in Table 2. The material was classified according to Model Code 2010 specifications [5] and denoted as “2.5c” with reference to the characteristic values.

## 3. SHALLOW BEAMS

Four nominally identical SFRC shallow beams 1.5 m long with a rectangular cross-section equal to 500×250 mm were realized the same day of the elevated slab casting and tested in a four-point bending test set-up (Fig. 2). Supports are 50 mm from the beam ends, while the displacements were imposed in sections situated 500 mm from the supports (Fig. 2). The shallow beams are named A, B, E, F, respectively. Two additional preliminary shallow beams named C and D having the same

geometry of the previous ones, but a different fiber content ( $30 \text{ kg/m}^3$ ) were tested on the same test set-up. The tests were carried out under displacement control by using the stroke displacement as feedback parameter. The deflection in the mid-span was measured through two (front and rear sides) Linear Variable Displacement Transducers (LVDT), while four transducers were applied in the beam central zone (3 on the bottom surface and one located on the top surface) to measure the crack opening displacement.

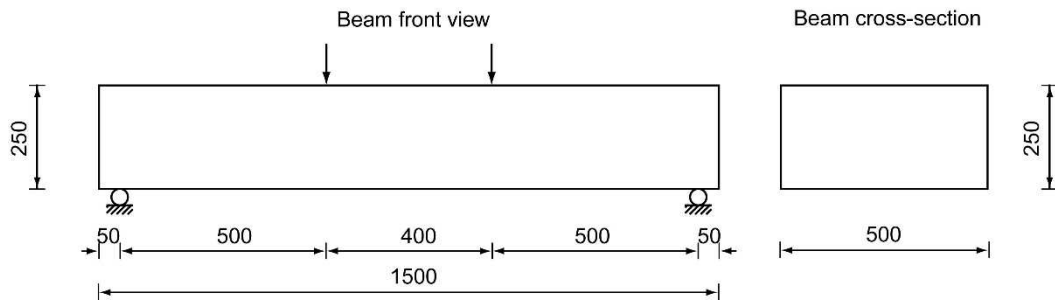


**Figure 2.** Dimensions (in mm) and test set-up for the shallow beams.

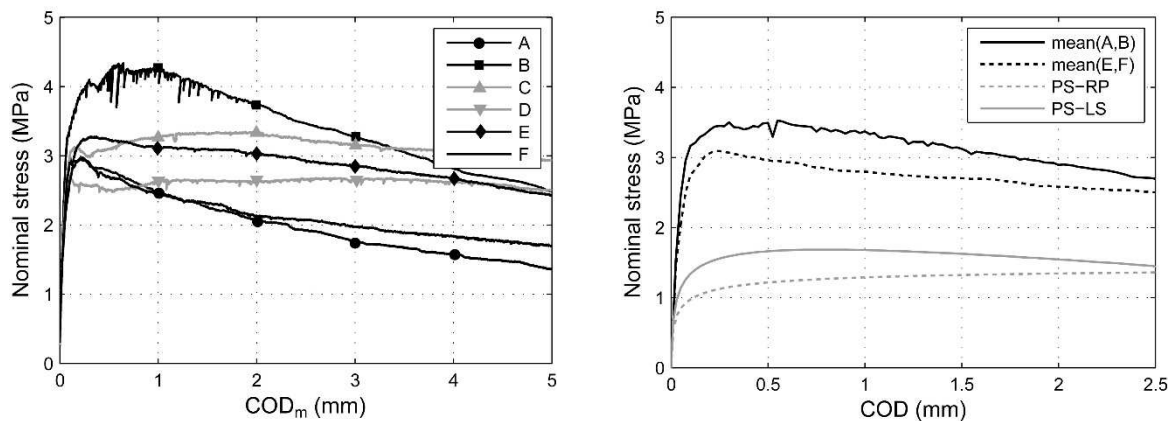


**Figure 3.** (a) Structural beam response in terms of nominal stress vs average COD for shallow beams A–F. (b) Average experimental responses and design plane section models based on rigid–plastic (PS–RP) and linear–elastic linear–softening (PS–LS) stress–crack opening constitutive laws for the shallow beams.

Figure 3a shows the response of the six beams in terms of nominal stress versus average crack opening displacement ( $\text{COD}_m$ ). This last is calculated as the average of the three transducers located on the bottom surface of the beams. The two preliminary beams C and D (in grey in Fig. 3a) are also included for comparison purpose. Shallow beams E and F were tested after a rotation of  $180^\circ$  along their longitudinal axis. This procedure was followed to investigate fiber segregation role in the mechanical response of the beams. In fact, fiber segregation could positively affect structures subjected to bending since it concentrates higher quantity of fibers at bottom layer.

The beam mechanical response is characterized by a large scattering with a COV of about 40% for beams A and B, and equal to 24% for beams E and F calculated at COD equal to 2.5 mm. This trend was to be expected since the loading scheme of the beams is statically determinate with a limited possibility of stress redistribution.

Limiting the attention to the final beams A, B, E and F, Figure 3b shows the response of the beams in terms of nominal stress vs  $\text{COD}_m$  calculated as the average values between beams A and B and between E and F, where the last two beams were tested after a rotation of  $180^\circ$  along their

longitudinal axis. The slightly lower curve for beams E and F compared to beams A and B indicates that fiber segregation played a not negligible role in the mechanical response.

The reliability of the design approach proposed in Model Code 2010 [5] for the estimation of the ultimate capacity of the SFRC shallow beams is assessed on the base of standard three–point bending test for material characterization combined with a multi–layer plane section approach.

The Model Code proposes two simplified models to describe the FRC response in tension after cracking, emphasizing the fiber pull–out effect: (a) the rigid–plastic and (b) the linear–elastic linear–softening models. The first model requires the identification of only one parameter,  $f_{Ftu}$  while the second requires the identification of two parameters  $f_{Fts}$  and  $f_{Ftu}$ , being  $f_{Fts}$  the serviceability residual strength, defined as the post–cracking strength for a crack opening significant for SLS and  $f_{Ftu}$  residual strength significant for ULS. Both  $f_{Fts}$  and  $f_{Ftu}$  are calculated using the residual flexural strengths  $f_{R1}$  and  $f_{R3}$  identified in bending; the complete derivation can be found in [11]. Starting from the material class (“2.5c”), it is possible to derive the design values  $f_{R1d}$  and  $f_{R3d}$  by dividing the characteristic values for the material safety factor  $\gamma_f$  equal to 1.5 according to [5].

A multi–layer plane section approach [12] is then used to calculate the beam response in terms of nominal stress versus COD. A linear strain distribution over the cross–section is assumed and the cross–section is discretized into several layers. A parabola rectangular constitutive model is adopted in compression while, a rigid–plastic or a linear–elastic linear–softening constitutive laws are considered for uniaxial tensile behavior as suggested by Model Code 2010 [5]. The structural characteristic length adopted is the beam depth since no steel reinforcement is included.

The specific ultimate bending moment is computed by imposing both translational and rotational equilibrium of the cross–section and assuming that the ultimate crack opening ( $w_u$ ) is reached at the bottom layer. In the present case an ultimate crack opening equal to  $w_u = 2.5$  mm was chosen according to [5].

Figure 3b compares the average beam experimental responses with the design results obtained through a multi–layer plane section approach. The rigid–plastic assumption provides the most conservative result compared to the response obtained by a linear–elastic linear–softening model.

#### **4. DOUBLE PUNCHING (BARCELONA) AND DOUBLE EDGE WEDGE SPLITTING (DEWS) TESTS**

The material post–cracking tensile behavior was also investigated by double edge wedge splitting (DEWS) and double punching (Barcelona or BCN) tests [7, 8]. The DEWS experimental testing technique allows to obtain directly the tensile stress versus crack opening “constitutive relationship”, while the BCN technique provides tensile stress vs the total crack opening displacement that divided by the number of cracks formed on the specimen gives the crack opening constitutive relationship of the material. Both tests are indirect tensile test where the tensile material behavior is obtained by applying a compressive load to the specimen. The description of these novel experimental techniques as well as their advantages compared to direct tension test and bending tests are widely discussed in [7] and in [8], respectively. The tests reveal attractive for their simplicity and straightforwardness of the identification procedure. DEWS and BCN tests have the peculiarity to use compact specimen geometry, which can be even easily cored from existing structures. Moreover, in the DEWS test a “notch preordained” fracture plane can be assigned to the specimen, so that the plane can be aligned to any desired angle with respect to the expected flow–induced fiber orientation. On the contrary BCN test allows an isotropic measure of the toughness giving a nominal stress vs crack opening as average on at least three radial cracked plane propagated after the penetration of two concrete cones formed in proximity of the two bases.

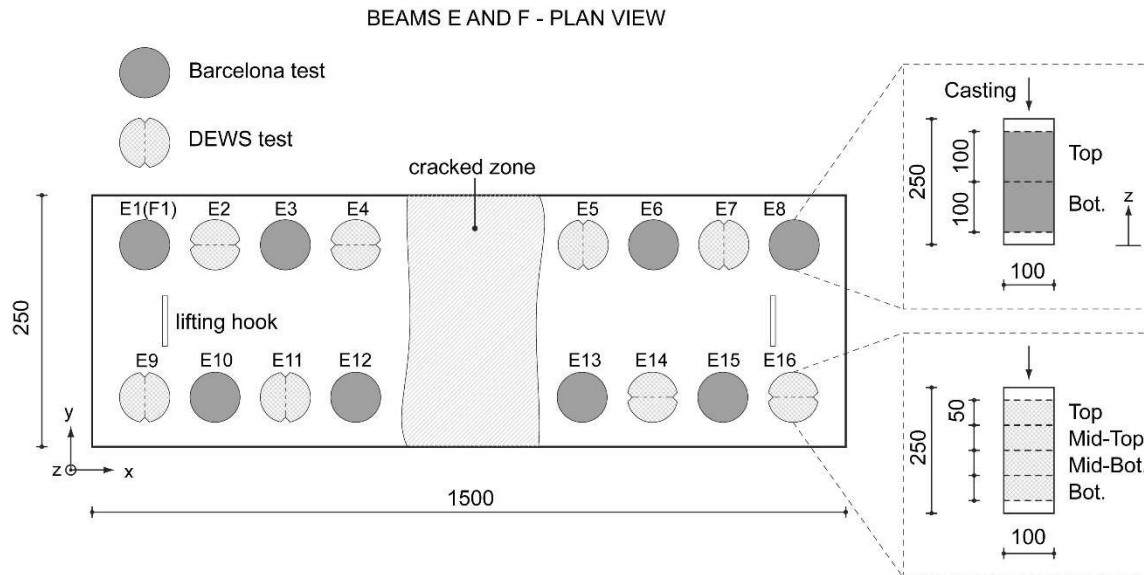


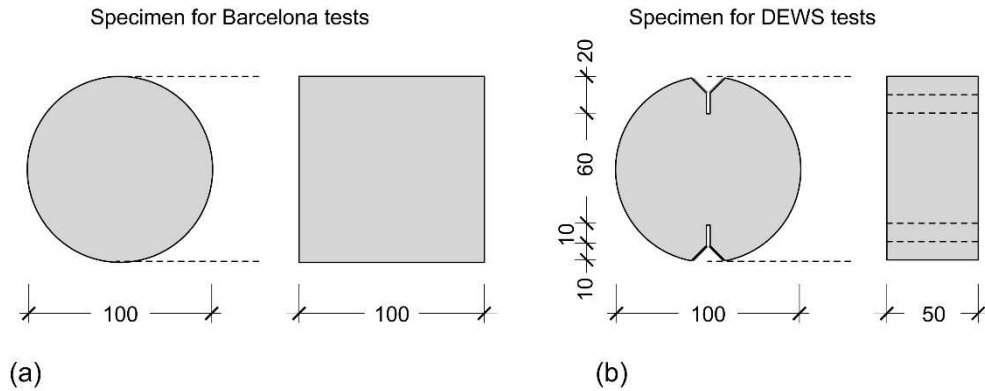
**Figure 4.** Position and size of the cylindrical cores extracted from the shallow beams E and F (dims. in mm).

After the shallow beam tests, forty-eight cylinders with a diameter of 100 mm were cored from the four beams along x, y and z directions (Figures 4 and 5). Cylinders cored along the beam thickness (z direction) have a length of 250 mm while the cylinders cored from x and y directions have a length of 400 mm. All the cylinders cored were never cracked in their volume. Shallow beams E and F were cored in z direction (Fig. 4), while beams A and B were cored in x and y directions (Fig. 5). Specimens employed for BCN tests were obtained by cutting cylinders cored in z direction in two equal parts and cylinders cored in x and y directions in three equal parts resulting in cylinder having a thickness of 100 mm. On the other hand, specimens employed for DEWS tests were obtained by cutting cylinders cored in z direction in four equal parts and cylinders cored in x and y directions in six equal parts resulting in cylinder having a thickness of 50 mm. From eight of the forty-eight original cylinders, 24 specimens having a thickness of 100 mm were prepared to be tested in direct tension in a forthcoming experimental campaign.

The total number of DEWS tests is equal to 112 (24 x-dir. + 24 y-dir. + 64 z-dir.), while the total number of BCN tests is equal to 56 (12 x-dir. + 12 y-dir. + 32 z-dir.). Specimen sizes are schematically indicated in Figure 6. The DEWS specimens have a 10 mm deep notch originating from the groove vertices. The DEWS tests were carried out at Politecnico di Milano by means of an electromechanical press (Instron 5867) with a bearing capacity of 30 kN and a precision equal to 0.4% and controlling the displacement of the actuator at a speed ranging from 0.5 to 1.0  $\mu\text{m/s}$ , as a function of the crack propagating stage. The crack propagation was detected through two LVDT placed at the mid-height of the specimen on front and rear sides. The BCN tests were carried out at the Universitat Politècnica de Catalunya using a hydraulic press (Ibertest) and a circumferential chain to measure the total crack opening displacement (TCOD). This test consists basically in a displacement – controlled ( $0.5 \pm 0.05$  mm/min) double punch test performed by placing two cylindrical steel punches (25 mm and 37.5 mm of height and diameter, respectively) above and below the cylindrical specimens ( $\Phi$  100 mm  $\times$  100 mm).

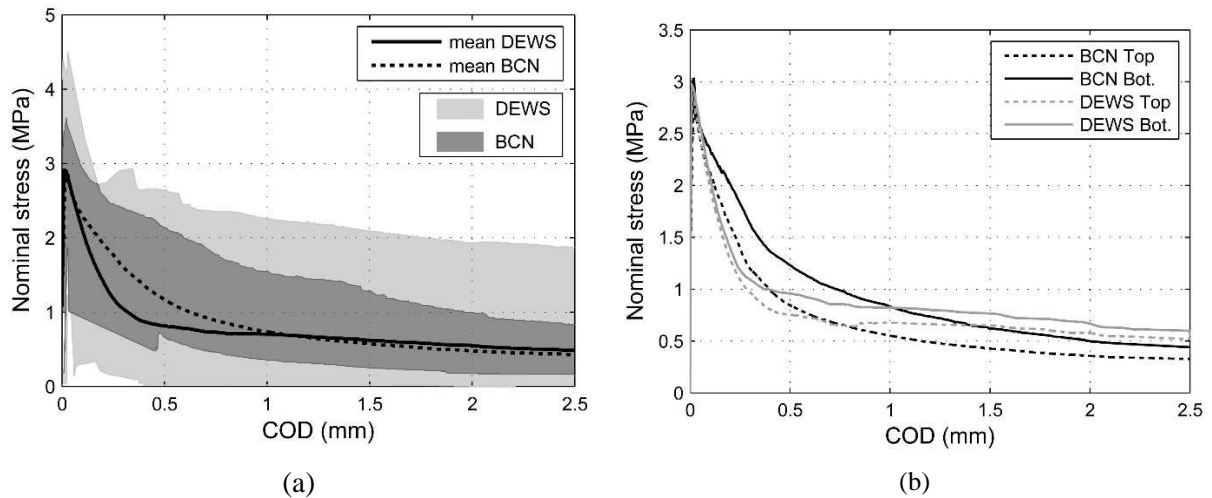
A univocal name distinguishes each specimens: the name starts with a letter indicating the cored beams followed by a progressive number indicating the position. An abbreviation name “Top”, “Mid-Top”, “Mid-Bot.” and “Bot.” or simply “Top”, and “Bot.” univocally identify respectively the DEWS and BCN position of the specimen inside the original cylinder core extracted along the beams thickness (for example “E3-Top”, etc.). The abbreviations “Top” and “Bot.” indicate respectively the top and bottom surfaces of the beams (Fig. 4).





**Figure 6.** Specimen dimension in mm for (a) Barcelona and (b) DEWS tests.

The two mean curves in Figure 7a shows peak points that are practically coincident. This is not surprising since it depends exclusively by plain concrete strength. Moreover, very similar trends between the two curves can be also observed in the fiber pull-out region (COD larger than 1 mm). This result is extremely interesting because when cracks appear and stabilize, the two experimental testing techniques lead to very similar material tensile behavior. The main difference between the two curves is observable in the initial softening branch after the peak stress. Immediately after the peak, the fibers are not yet activated and the tensile behavior is governed by the concrete matrix. DEWS curve is characterized by a higher slope compared to the BCN curve. This means that the energy released in the BCN test immediately after the peak stress is higher than the one released in the DEWS and is mainly due to the friction energy associated to the formation of the conical wedges.



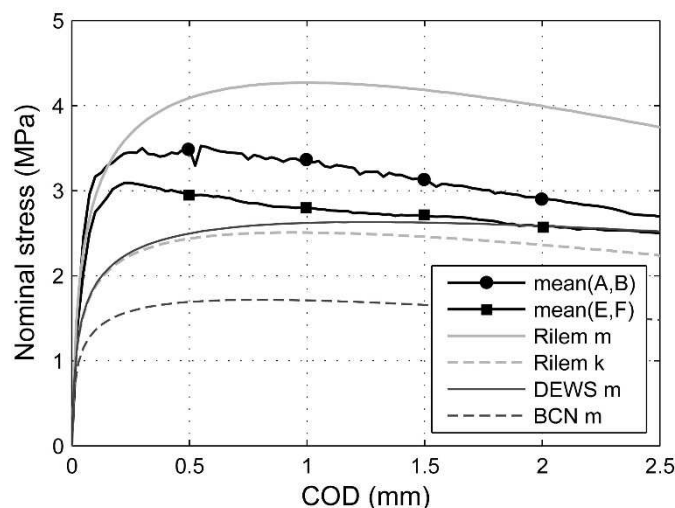
**Figure 7.** (a) Nominal stress vs COD from DEWS and BCN tests: average values and scattering obtained considering the total number of specimens. (b) Influence of the specimens position along the thickness in terms of nominal stress versus COD for the BCN and DEWS tests (Top = casting side; Bot. = formwork side).

Figure 7a shows as the scattering of the two methods is very different. BCN tests provides a COV equal to 26% and 34% for a COD equal to 0.5 and 2.5 mm, respectively, while DEWS gives a COV equal to 69% and 76% for a COD equal to 0.5 and 2.5 mm, respectively. This difference can be justified by the different areas involved in the cracked process for the two testing methods. For BCN the cracked area is about  $A_{BCN} = 42 \times 3 = 126 \text{ cm}^2$ , while for DEWS the cracked area is  $A_{DEWS} = 5 \times 6 = 30 \text{ cm}^2$ , with a ratio  $A_{BCN}/A_{DEWS} \cong 4$ . An important aspect related to the casting of FRC element is the possible fiber segregation. To this regards, a recent study has pointed out the occurrence of fiber segregation in an elevated slab [4]. It is possible to analyze the fiber segregation by considering the

specimen cored along the thickness ( $z$ -direction) and subdividing the specimen in contact with the formwork (“Bot.” specimens) from the specimens facing the casting surface (“Top” specimens). Figure 7b compares all “Top” and “Bot.” specimens tested with BCN and DEWS techniques. The results indicate that fiber segregation took place during the casting phase. The specimens in contact with the formwork perform better, in average sense, than the specimens facing the casting surface.

On the base of the BCN and DEWS results, it is possible to simulate the shallow beams behavior by a multi-layer plane section approach. The FRC response in tension after cracking is described with a linear-elastic linear-softening models according to the Model Code proposal [5]. The two parameters necessary to identify the tensile constitutive law are directly deduced considering the nominal stress at 0.5 and 2.5 mm of COD. For the BCN tests, the nominal stress at COD equal to 0.5 mm is obtained by a linear interpolation using the experimental values at COD of 1.5 and 2.5 mm to overcome the problem related to the spurious energy due to the formation of the conical wedge previously described. Then for both the techniques, the stress measured (or extrapolated) to a COD of 0.5 mm has been associated to a COD equal to zero for the construction of the constitutive law as suggested by [11]. In order to better simulate the flexural behavior of the beam, only the DEWS specimens with cracked plane orthogonal to the beam  $x$ -axis are considered (i.e. cores E5, F5 and E11, F11 for a total of 16 specimens). For the BCN specimens is not possible to pre-assign a fracture plane as already discussed in Section 3: therefore only the cylinders cored in  $z$ -direction (E3, F3; E6,F6; E12, F12; E13,F13) have been considered. The selection was made in order to be not affected by wall effects at the ends.

The experimental and numerical beam responses are compared in Figure 8 adopting for the plane section approach mean values of the selected DEWS and BCN specimens. The BCN results, which includes fracture planes not necessarily orthogonal to beam  $x$ -axis, provide the most conservative results. For the same reasons, BCN specimens could not be very precise into simulating the boundary conditions induced by wall effects of formworks. The selected DEWS specimens are closer to the mean experimental beam results compared to the BCN ones and both testing techniques provide safe predictions. Finally, the numerical response obtained adopting the mean results of the Rilem tests is included in Figure 8 for comparison purpose. It overestimates the experimental mean response confirming the need of characteristic and design value adoption if a structure has a limited capacity to redistribute the stresses, as for the statically determinate shallow beams herein considered [13].



**Figure 8.** Average experimental responses for the shallow beams and plane section model (linear-elastic linear-softening ) based on Rilem, DEWS and BCN results.

## 5. CONCLUSIONS

A 240 m<sup>2</sup> SFRC elevated slab was designed and built in a two-storey family house in Erba. The bending characterization indicated a “2.5c” class for the SFRC material. The Model Code 2010 approach used to predict the behavior of two bent shallow beams made of the same material and without any traditional reinforcement confirms the reliability of the approach. By coring the shallow beams, the constitutive models suggested by Model Code are compared with the results of two other simplified tests based on indirect tension: Barcelona test confirms its reliability for production control and DEWS test appears very effective to evaluate the effects of fiber orientation.

## ACKNOWLEDGMENTS

Stampini construction company and Calcestruzzi Erbesi concrete producer financially supported the research programme. The authors are also in debt with DSC–Erba Company Design for the assistance in the specimen preparation and the access to the design drawings.

## REFERENCES

- [1] Mobasher, B., & Destrée, X. (2010) Design and construction aspects of steel fiber-reinforced concrete elevated slabs. *American Concrete Institute, ACI Special Publication*, (274 SP), 95-107.
- [2] Hedebratt, J., & Silfwerbrand, J. (2014) Full-scale test of a pile supported steel fibre concrete slab. *Materials and Structures/Materiaux et Constructions*, 47(4), 647-666.
- [3] di Prisco, M., Plizzari, G., & Vandewalle, L. (2014) Structural design according to fib MC 2010: comparison between RC and FRC elements. In: *FRC 2014 Joint ACI-fib International Workshop - Fibre Reinforced Concrete: from Design to Structural Applications*, Editors: Charron J.P., Massicotte B., Mobasher B., Plizzari G., Montreal, Canada.
- [4] di Prisco, M., Martinelli, P., & Parmentier, B. (2016) On the reliability of design approach for FRC structures according to Model Code 2010: the case of elevated slabs. *Structural Concrete*, DOI: 10.1002/suco.201500151
- [5] fib Model Code for Concrete Structures 2010 (2013) Fédération Internationale du Béton, Ernst & Sohn, Lausanne.
- [6] EN 14651, (2004) Test method for metallic fiber concrete – Measuring the flexural tensile strength (limit of proportionality, residual).
- [7] di Prisco, M., Ferrara, L., & Lamperti, M.G.L. (2013) Double edge wedge splitting (DEWS): An indirect tension test to identify post-cracking behaviour of fibre reinforced cementitious composites. *Materials and Structures/Materiaux et Constructions*, 46(11), 1893-1918.
- [8] Molins, C., Aguado, A., & Saludes, S. (2009) Double punch test to control the energy dissipation in tension of FRC (Barcelona test). *Materials and Structures/Materiaux et Constructions*, 42(4), 415-425.
- [9] CEN EN 14721, (2005) Test method for metallic fibre concrete - Measuring the fibre content in fresh and hardened concrete - European Committee for Standardization, Brussels.
- [10] UNI EN 1990, (2006) Eurocode – Basis of structural design, European Committee for Standardization, Brussels.
- [11] di Prisco, M., Colombo, M., & Dozio, D. (2013) Fibre-reinforced concrete in fib Model Code 2010: Principles, models and test validation. *Structural Concrete*, 14(4), 342-361.
- [12] Hordijk, D. (1991) Local approach to fatigue of concrete. PhD thesis. Delft, delft University of Technology.
- [13] di Prisco, M., Martinelli, P., & Dozio, D. (2016) The structural redistribution coefficient KRd: a numerical approach to its evaluation. *Structural Concrete*, DOI: 10.1002/suco.201500118.